

See discussions, stats, and author profiles for this publication at: <https://www.researchgate.net/publication/231665609>

Infrared Spectroscopic Observation of the Stabilized Intermediate Complex FO₃ Formed by Reaction of Mobile Fluorine Atoms with Ozone Molecules Trapped in an Argon Matrix

ARTICLE in THE JOURNAL OF PHYSICAL CHEMISTRY A · SEPTEMBER 1999

Impact Factor: 2.69 · DOI: 10.1021/jp9921194

CITATIONS

14

READS

6

3 AUTHORS:



Eugenii Ya Misochko

Russian Academy of Sciences

65 PUBLICATIONS 525 CITATIONS

SEE PROFILE



Alexander Akimov

Russian Academy of Sciences

51 PUBLICATIONS 470 CITATIONS

SEE PROFILE



Charles A. Wight

Weber State University

141 PUBLICATIONS 3,610 CITATIONS

SEE PROFILE

Infrared Spectroscopic Observation of the Stabilized Intermediate Complex FO₃ Formed by Reaction of Mobile Fluorine Atoms with Ozone Molecules Trapped in an Argon Matrix

Eugenii Ya. Misochko,[†] Alexander V. Akimov,[†] and Charles A. Wight*

Department of Chemistry, University of Utah, Salt Lake City, Utah 84112

Received: June 24, 1999; In Final Form: August 6, 1999

Chemical reaction of F atoms with O₃ molecules in a solid argon matrix was studied with FTIR spectroscopy. Fluorine atoms were generated by UV photolysis of F₂ molecules in dilute solutions of F₂ and O₃ in solid argon. The FO–O₂ complex is observed for the first time as an intermediate product by reaction of mobile F atoms with isolated ozone molecules. The observed complex is characterized by two intense absorption bands at 1522 and 968 cm^{−1}. Use of isotopic mixtures ¹⁶O/¹⁸O provides strong evidence for assignment of these bands to the O–O stretch and F–O stretch fundamentals of the complex, which are red-shifted by 34 and 61 cm^{−1}, respectively, from the corresponding values for O₂ and FO. Photolysis at 532 nm leads to decay of the FO–O₂ complexes and to the appearance of isolated free FO radicals.

1. Introduction

The halogen oxides attract interest because of their important role in stratospheric chemistry and as strong oxidizing agents. In particular, since 1934, when chlorine trioxide was postulated as a reaction intermediate¹ as well as an unstable product in the chlorine photosensitized decomposition of ozone,² there have been several intensive investigations of the reactions of halogens and halogen oxides with ozone.^{3–9} Although much of this research lies in the area of reaction kinetics and stratospheric modeling, the role of long-lived intermediates such as asymmetric ClO₃ in the atmospheric ClO_x cycle remains poorly understood. To our knowledge, there is no direct experimental evidence of a loosely bonded asymmetrical ClO–O₂ association complex. Only the infrared and UV spectra of the symmetric C_{3v} structure of ClO₃ species were detected recently by the pyrolysis of chlorine perchlorate.⁹ Moreover, Carter and Andrews' matrix isolation study of the reaction Cl + O₃ showed no observable IR absorption of a possible asymmetric ClO₃ species.¹⁰ Among the four ClO₃ isomers, only the ground state (²A₁) C_{3v} structure was found to be stable in quantum chemistry calculations by Rauk et al.¹¹ Recently, Zhang et al.^{8,12} concluded from a crossed molecular beam study that the reactions Cl + O₃ and Br + O₃ proceed through a direct reaction mechanism, and an asymmetric covalently bound XO₃ complex (X = halogen) is unlikely to exist as a long-lived intermediate.

The oxygen fluorides, FO, FOO, FOF, OFO, and FOOF, have been studied both experimentally and using quantum chemistry calculations.¹³ In this paper we present the first experimental evidence of the association complex FO–O₂, produced by solid-state reaction of fluorine atoms with ozone molecules isolated in solid argon. Our experimental methodology is based on the widely used matrix isolation technique. It also takes advantage of the high mobility of fluorine atoms in crystalline argon at temperatures well below its melting point, as observed by

Apkarian et al.,^{14,15} who showed that translationally excited "hot" fluorine atoms formed by UV photolysis of F₂ molecules migrate through several lattice periods. The thermal F atoms are essentially immobile in the matrix at temperatures less than 18 K. However, at 20–26 K, F atoms are able to diffuse approximately 10 nm through argon in 10²–10⁴ s because the barrier to thermal diffusion of F atoms in solid argon is only 4.5–5.5 kJ/mol. The ability to control the mobility of F atoms provides a unique opportunity to carry out solid-state chemical reactions of F atoms with various molecules trapped in argon matrix. Yet, the crystalline environment prevents reaction products from flying apart and promotes fast relaxation of excess energy released in reaction. Therefore, the solid state permits the stabilization and spectroscopic characterization of intermediate species that are not observable in gas-phase studies.

Using this approach, we have recently determined the spectral characteristics of reactive intermediates formed by reactions of F atoms with ethene,¹⁶ methane,¹⁷ hydrogen,¹⁸ carbon monoxide,¹⁹ oxygen,¹⁹ and nitric oxide.²⁰ In the present study, we have detected by FTIR spectroscopy the stabilized complex FO–O₂ in dilute mixtures of F₂ and O₃ in solid argon using F₂ as a photolytic precursor of F atoms. These results may serve as a starting point for quantum chemistry calculations in an effort to understand the nature of the chemical bonding in this complex and the topology of the potential energy surface in the vicinity of the transition state of atom–molecule reactions of the type X + O₃ → XO + O₂.

2. Experimental Details

The experimental techniques are similar to those used in our previous study.¹⁶ Dilute mixtures of F₂:Ar and O₃:Ar are deposited through separate stainless steel vacuum manifolds onto the surface of a CsI window held at 15 K in a high-vacuum chamber. The sample chamber is constructed of polished stainless steel and ultrahigh-vacuum flanges. It is pumped by a 50 L/s turbomolecular pump; the base pressure of this apparatus is typically 5 × 10^{−5} Pa. A portion of the stainless steel deposition line for F₂/Ar gas mixture was immersed in liquid nitrogen during sample deposition in order to remove impurities

[†] Permanent address: Institute of Problems of Chemical Physics of the Russian Academy of Sciences, 142432, Chernogolovka, Moscow Region, Russia.

* To whom correspondence should be addressed.

formed by reactions in the manifold. In all of the experiments, the mole fraction of reactants (F₂ and O₃) was less than 5×10^{-4} . The gases oxygen, argon (Spectra gases, 99.999%), and fluorine (Spectra gases, 10% in Ar) were used without further purification. Ozone is prepared from oxygen by Tesla coil discharge and trapping in a cold glass finger immersed in liquid nitrogen. Each ozone sample is purified by several freeze-pump-thaw cycles. The sample preparation manifold is passivated by allowing a few Torr of ozone to rest in the line prior to preparation. In some experiments ozone was prepared with isotopically enriched O₂ (¹⁶O:¹⁸O \approx 3:2).

Fluorine atoms were generated by F₂ photolysis at 355 nm with the third harmonic of a Nd:YAG laser (Continuum model Surelite). The absorption cross section of F₂ at this wavelength is 1.1×10^{-20} cm². The laser light entered the sample chamber through a fused silica window and impinged on the sample at an incident angle of 45°. The beam was expanded to an area of about 3.5 cm² at the sample to ensure uniform irradiation. The average laser power was varied from 1 to 10 mW/cm². In some experiments, we used the second harmonic of a Nd:YAG laser at 532 nm at an average laser power of 20 mW/cm² for photolysis of the reaction products.

Freshly prepared samples of Ar/F₂/O₃ exhibited a weak band at 2139 cm⁻¹, due to impurity CO molecules formed in the manifold during deposition. We estimated the typical amount of this impurity in samples relative to the O₃ molecules, [CO]/[O₃] $\sim 2 \times 10^{-2}$, using the known IR absorption cross section of CO in solid argon.¹⁹ As it will be shown below, the impurity O₂ was also present in the samples. The O₂ is presumably formed by decomposition of O₃ in the manifold during sample preparation. On the basis of our earlier study of the samples Ar/F₂/O₂,¹⁹ we estimated the typical amount of this impurity in the samples, [O₂]/[O₃] $\sim 0.15 \pm 0.05$.

3. Results and Analysis

a. Photolysis of Solid Mixtures Ar:O₃ and Ar:F₂:O₃ at 15 K. Infrared spectra of ozone in the samples Ar:O₃ = 5000:1 and Ar:F₂:O₃ = 5000:3:1 are similar and are in good agreement with literature data for the O₃ molecules in an argon matrix.^{21,22} In additional experiments, we measured the integrated absorption cross section of the ν_3 fundamental band of ozone by a method described in detail elsewhere,²³ which is based on comparing the measured integrated infrared absorption with amount of O₃ molecules deposited per unit area on the sample window. The resulting value, $B(\nu_3) = 68 \pm 10$ km/mol, is close to the literature value for O₃ in a gas phase, 84 km/mol.^{24,25} Because part of the ozone decomposes in the manifold during sample preparation, it is necessary to regard the measured value as a lower limit of $B(\nu_3)$. Therefore, we have used both values below (in section 4), as the upper and lower limits of $B(\nu_3)$, in calculations of the reaction mass balance.

Isolation and photodecomposition of O₃ molecules in rare gas matrixes were studied earlier by Wight et al.^{22,26,27} It was shown that, at mole fractions of ozone molecules in argon higher than $x \sim 10^{-4}$, aggregation and clustering of ozone are significant. For example, at $x = 10^{-3}$, only 40% of the ozone molecules are present as monomers.²² Although the absorption cross section for O₃ molecules in the gas phase at 355 nm is very low (Huggins band)²⁸ relative to that for F₂ molecules, $\sim 10^{-22}$ cm², the ozone aggregates and clusters may have much higher absorption at this wavelength.^{22,29} To distinguish a photochemical processes induced by photodissociation of F₂ and O₃ molecules, we have performed photolysis in dilute Ar/O₃ samples.

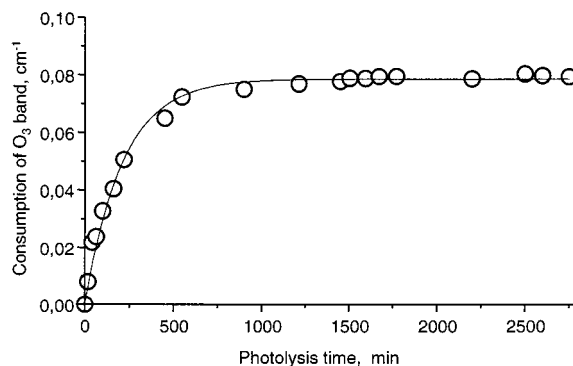


Figure 1. Consumption of the integrated absorption of the ν_3 ozone band during 355 nm photolysis of the sample Ar:O₃ = 5000:1 at 15 K. The average laser power is 2.5 mW/cm². The initial integrated absorption of ν_3 band was 0.79 cm⁻¹. The solid curve is the single-exponential fit to the data with characteristic time 220 min.

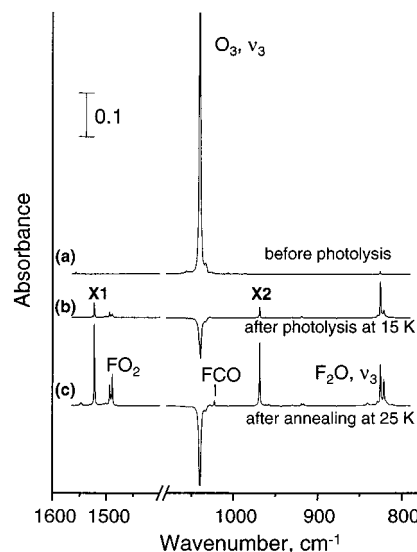
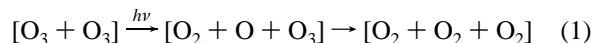


Figure 2. Infrared spectra of the sample Ar:F₂:O₃ = 5000:3:1 at 15 K. Trace a shows the structure of the O₃ band prior to photolysis. Trace b is a difference spectrum showing changes in the bands following 355 nm photolysis at 15 K. Trace c is a difference spectrum showing the additional changes that occur during annealing of the sample at 25 K.

Figure 1 shows kinetics of consumption of O₃ during photolysis of the sample Ar:O₃ = 5000:1 at 15 K. After exhaustive photolysis the integrated intensities of the IR ozone bands decreased by 10%. No new lines of photolysis products were detected.

Ozone in clusters and aggregates are known to undergo photodecomposition by a two-step chain pathway²²



producing oxygen molecules, which are IR-inactive. The observed 10% consumption of ozone in the samples Ar:O₃ = 5000:1 is therefore due to the presence of ozone aggregates that are destroyed in reaction 1. The remaining 90% of O₃ molecules, which are isolated in argon, are not decomposed at 355 nm to any significant extent.

The infrared spectrum of a freshly prepared sample Ar:F₂:O₃ = 5000:3:1 in the region of the ν_3 fundamental of ozone is shown in Figure 2. This band exhibits two narrow peaks at 1041 and 1049 cm⁻¹, which correspond to two different sites occupied by ozone molecules in the argon lattice. Photolysis of samples at 15 K yields an intense doublet band at 825 and 821 cm⁻¹

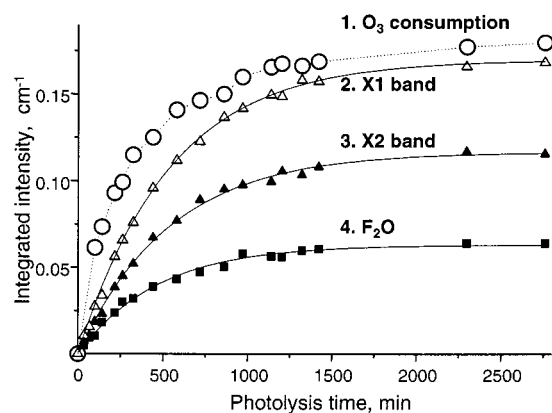


Figure 3. Kinetic plot of the integrated IR band intensities of the X1 band at 1522 cm^{-1} (curve 2), the X2 band at 968 cm^{-1} (curve 3), and F_2O at 825 cm^{-1} (curve 4) during 355 nm photolysis of the sample $\text{Ar}:\text{F}_2:\text{O}_3 = 5000:3:1$ at 15 K. Curve 1 shows consumption of the ν_3 ozone band. The initial integrated absorption of the ν_3 band was 0.81 cm^{-1} . The solid curves are single-exponential fits to the data (2) and (3) with characteristic time $\tau = 560$ min and to the data (4) with $\tau = 430$ min.

and very weak band at 925 cm^{-1} . These bands were definitively assigned to the ν_3 and ν_1 fundamentals of the F_2O molecule.^{30–32} A relatively weak band at 1490 cm^{-1} corresponds to the FO_2 radical. This radical appears in the reaction of F atoms with O_2 molecules, as shown in our previous study.¹⁹ Photolysis also produces two intense infrared bands at 1522 and 968 cm^{-1} , which are labeled in Figure 2 as X1 and X2, respectively. These two bands never appear upon photolysis of the samples Ar/F_2 , Ar/O_3 , and $\text{Ar}/\text{F}_2/\text{O}_2$. Figure 3 shows the kinetics of consumption of O_3 molecules and the growth of the ν_2 band of F_2O , X1 and X2 upon photolysis. After an extended photolysis period the integrated intensity of the ozone band decreases by 22%; i.e., consumption of ozone is 2 times greater than in the sample $\text{Ar}:\text{O}_3 = 5000:1$ containing the same initial amount of O_3 molecules (see Figure 1). The solid curves in Figure 3 are single-exponential fits to the experimental data. The products bands X1 and X2 grow at the same rate, whereas the production of F_2O molecules occurs with a significantly faster photochemical reaction rate.

b. Annealing of the Samples $\text{Ar}/\text{F}_2/\text{O}_3$ Photolyzed at 15 K.

To initiate reaction of thermal F atoms, we performed annealing of the photolyzed samples at 25 K. Annealing was carried out by step-by-step procedure. After completion of photolysis at 15 K, the sample was annealed 3–5 min at 25 K. Then the temperature was lowered back to 15 K, and an IR spectrum was recorded. This cycle was repeated 12–15 times until the reaction was complete. Changes in the IR spectra upon annealing of the sample are illustrated in Figure 2. Growth of the product bands, labeled as X1 and X2, and decrease of ozone band account for the major changes in the initial stages of annealing. Simultaneously, growth of two smaller series of bands 1490, 1153, 584 cm^{-1} and 1857, 1023, 628 cm^{-1} , corresponding to the stabilized radicals FO_2 and FCO , respectively, takes place. These radicals are formed by addition reactions of diffusing F atoms with impurity molecules O_2 and CO ,



as was shown in our previous paper.¹⁹

In the final stages of annealing, growth of bands assigned to the F_2O molecules is dominant. The total consumption of O_3

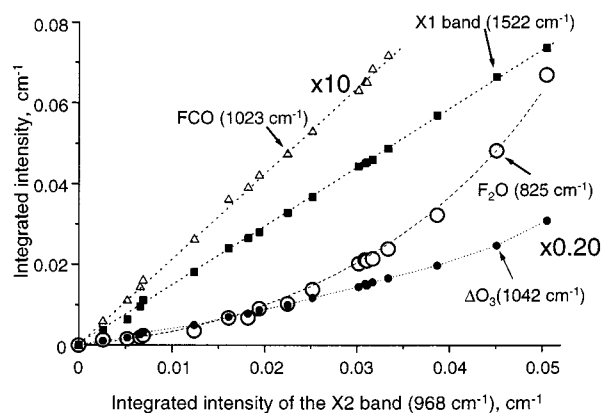


Figure 4. Growth of the product bands and consumption of the ozone band vs intensity of the X2 product band during annealing of the photolyzed sample $\text{Ar}:\text{F}_2:\text{O}_3 = 5000:3:1$.

molecules after annealing cycles in the samples $\text{Ar}:\text{F}_2:\text{O}_3 = 5000:3:1$ may run as high as 50% relative to the amount of O_3 molecules before annealing. The growth of the major product bands and decrease of the O_3 band upon annealing of the sample are shown in Figure 4. Here, the intensities of product bands X1, X2, and FCO each exhibits a linear relationship to the diminution of the ozone band. The linear relationship of these changes in intensity shows that these species are primary reaction products of diffusing F atoms with isolated molecules (O_3 or CO) in the argon lattice. In contrast, the growth of F_2O , which requires two F atoms, exhibits a second-order nonlinear relationship to the other bands. This kinetic observation, that X1 and X2 belong to a species that is a primary $\text{F} + \text{O}_3$ reaction product, is an important clue to its identification.

It is well-known that reaction of an F atom with O_3 produces the FO free radical and O_2 molecule in the gas phase. The IR absorption band of FO free radical lies at 1033 cm^{-1} in the gas phase. For FO radicals isolated in an argon matrix, this IR absorption band lies at 1029 cm^{-1} . The X2 product band lies fairly close to that of FO but exhibits a red shift of 61 cm^{-1} relative to the FO radical isolated in solid argon.^{30–32} Likewise, the X1 product band lies fairly close to that of O_2 but exhibits a 34 cm^{-1} red shift relative to the gas-phase O_2 fundamental at 1556 cm^{-1} .³³ Moreover, the X1 band has a considerable infrared absorption cross section, whereas the gas-phase O_2 vibration is IR-inactive.

This comparison leads to the conclusion that the X1 and X2 bands can be assigned to a strongly interacting stabilized complex $\text{FO}-\text{O}_2$, in which each half of the complex is significantly perturbed relative to the corresponding free diatomic molecule. As the isotopic effect is a very helpful tool to identify reliably the vibrational bands, we have performed similar experiments with ^{18}O -enriched ozone samples.

c. Annealing of the Photolyzed Samples Containing Isotopes ^{16}O and ^{18}O . Because we used oxygen mixtures containing isotopes ^{16}O and ^{18}O for preparing ozone molecules, all the isotopic combinations of O_3 were observed in the ν_3 region of the samples Ar/O_3 and $\text{Ar}/\text{F}_2/\text{O}_3$ as shown in Figure 5, which are in good agreement with literature data.²¹ Changes in the IR spectra upon annealing of the photolyzed sample $\text{Ar}/\text{F}_2/\text{O}_3$ are shown in Figure 6. It demonstrates consumption of all of the isotopic components of ozone upon annealing. In the region of the $\text{O}-\text{O}$ stretch vibration, the spectrum contains two new components at 1480 and 1436 cm^{-1} along with the X1 band at 1522 cm^{-1} . The relative intensities of these three bands correspond to the relative amount of the isotopic combination $^{18}\text{O}^{18}\text{O}$, $^{16}\text{O}^{18}\text{O}$, and $^{16}\text{O}^{16}\text{O}$ in the sample, respectively. The

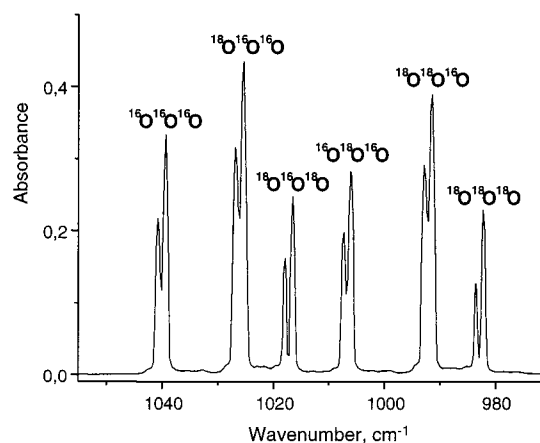


Figure 5. Absorption of the ν_3 mode of ^{18}O -substituted ozone in the sample $\text{Ar}:\text{O}_3 = 5000:1$ at 15 K.

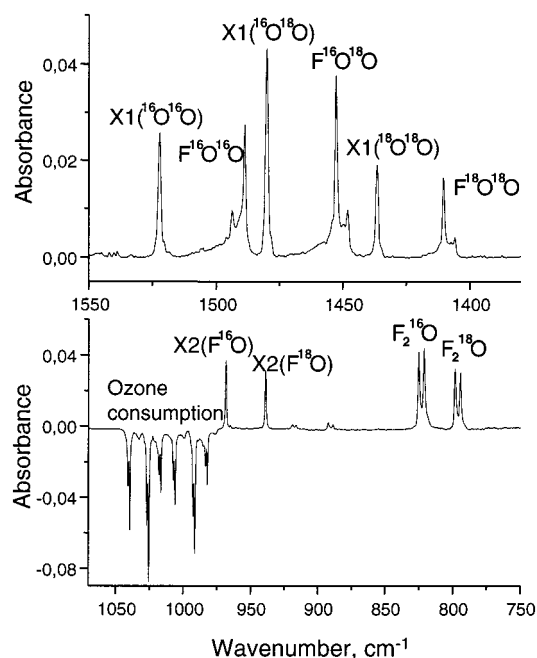


Figure 6. Difference infrared spectra of the ^{18}O -enriched sample ($^{16}\text{O}:\text{O}_3 \approx 3:2$) $\text{Ar}:\text{F}_2:\text{O}_3 = 5000:3:1$ at 15 K. The experimental conditions correspond to trace c in Figure 2.

TABLE 1: Absorption Bands Produced by Annealing of the Photolyzed Samples $\text{Ar}:\text{F}_2:\text{O}_3(\sim 40\% \text{ } ^{18}\text{O}) = 5000:3:1$

$\nu_{\text{obs}} (\text{cm}^{-1})$	vibrational assignment
1522.2	X1, ($^{16}\text{O}-^{16}\text{O}$)
1480.0	X1, ($^{16}\text{O}-^{18}\text{O}$)
1436.3	X1, ($^{18}\text{O}-^{18}\text{O}$)
1493.7, 1488.8	$\text{F}^{16}\text{O}^{16}\text{O}$
1452.7, 1448.0	$\text{F}^{16}\text{O}^{18}\text{O}$ (and $\text{F}^{18}\text{O}^{16}\text{O}$)
1410.3, 1405.8	$\text{F}^{18}\text{O}^{18}\text{O}$
968.4	X2, ($\text{F}-^{16}\text{O}$)
938.9	X2, ($\text{F}-^{18}\text{O}$)
825.2, 821.1	F_2^{16}O
798.2, 794.2	F_2^{18}O

spectrum also contains three doublet bands corresponding to the O—O stretch of the FO_2 radical³⁴ (see Table 1). In the region of the F—O stretching vibration, the spectrum contains one new component at 939 cm^{-1} along with the X2 band at 968 cm^{-1} . The relative intensities of these two bands correspond to the relative amount of the isotopes ^{18}O and ^{16}O in the sample. The spectrum also contains two doublet bands of F_2O products, which are listed in the Table 1.

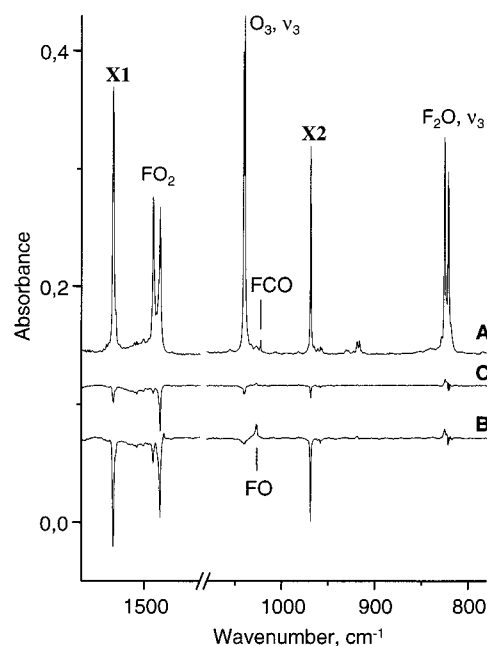
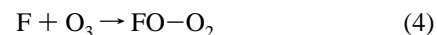


Figure 7. Infrared spectra of the sample $\text{Ar}:\text{F}_2:\text{O}_3 = 5000:3:1$ at 15 K. Trace a shows the spectrum after 355 nm photolysis at 15 K and subsequent annealing at 25 K. Traces b and c are difference spectra showing changes in the bands following 5 and 80 min 532 nm photolysis at 15 K.

The observed isotopic shift for the two X2 bands, $\Delta\nu = 29.5 \text{ cm}^{-1}$, is in good agreement for that calculated for a pure FO vibration, 29.7 cm^{-1} , where the vibrational frequency is inversely proportional to the square root of the reduced mass of the two atoms.

The fact that the spectrum contains three X1 bands (corresponding to three isotopic combination $^{16}\text{O}^{16}\text{O}$, $^{16}\text{O}^{18}\text{O}$, and $^{18}\text{O}^{18}\text{O}$) is definitive evidence of an O—O vibration. The observed isotopic shifts $\Delta\nu_1 = \nu(^{16}\text{O}-^{16}\text{O}) - \nu(^{16}\text{O}-^{18}\text{O}) = 42.2 \text{ cm}^{-1}$ and $\Delta\nu_2 = \nu(^{16}\text{O}-^{16}\text{O}) - \nu(^{18}\text{O}-^{18}\text{O}) = 85.9 \text{ cm}^{-1}$ are in agreement with calculated values for a pure O—O vibration (42.9 and 87.0 cm^{-1} , respectively). Thus, these data allow to conclude unambiguously that the product bands X1 and X2 correspond to the O—O and F—O vibrations, respectively, and the strongly interacting stabilized complex $\text{FO}-\text{O}_2$ is the main reaction of F atoms with O_3 molecules in a solid argon matrix:



d. Photolysis of the Reaction Products at 532 nm Laser Light. To test the photostability of the $\text{FO}-\text{O}_2$ complex to visible light, a sample containing the reaction products was subjected to irradiation by 532 nm laser light. The resulting spectra are shown in Figure 7. The initial stage of photolysis causes a decrease of the bands of the FO_2 radical. As was established earlier by Jacox,³⁴ photodecomposition of the radicals FO_2 with light at $\lambda < 400 \text{ nm}$ could arise from the following reaction channel

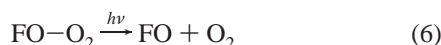


yielding IR-inactive products. Extended photolysis leads also to a decrease of both X1 and X2 bands of the complex $\text{FO}-\text{O}_2$. Photolysis produces only one new band at 1029 cm^{-1} which is due to isolated FO radical in argon.^{30–32} Growth of intensity of this band occurs simultaneously with the diminution of the X1 and X2 bands during photolysis. Such correlation provides

TABLE 2: Consumption of Ozone Molecules and Accumulation of Products after Exhaustive Photolysis of a Sample Ar:F₂:O₃ = 5000:3:1 at 15 K (Relative to the Initial O₃ Content)

1. consumption of O ₃	0.225
2. accumulation of FO—O ₂	0.035
3. accumulation of F ₂ O	0.113
photolysis of clusters of O ₃	0.225 − 0.035 − 0.113 = 0.077

the basis to conclude that the complex FO—O₂ absorbs light at 532 nm and decomposes to FO and O₂.



A direct comparison of the decrease in X2 band intensity (at 968 cm^{−1}) and the increase in isolated FO molecule band intensity (at 1029 cm^{−1}) shows that the absorption cross section for the F—O band in the complex is ~3 times larger than that for the isolated FO molecule.

4. Discussion

The main experimental result of the present study is that the reaction F + O₃ in solid argon produces the strongly interacting stabilized complex FO—O₂. Even without the detailed kinetic analysis, the experimental results (i.e., isotopic substitution and photolysis of the reaction products by 532 nm laser light) provide definitive evidence for this conclusion. Below we shall consider the reaction channels giving the two main products: the FO—O₂ complexes and F₂O.

a. Reactions of Photogenerated “Hot” F Atoms at 15 K.

As follows from our previous studies,^{17,19} usually there are two types of reactants in a solid matrix-deposited mixtures Ar/F₂/M (where M is the reactant molecule): isolated (spatially separated) F₂ and M molecules and the van der Waals complexes of reactants F₂—M. Though it is not always possible to detect such complexes of reactants by IR spectroscopy, they are always present in samples prepared under the given experimental conditions. Photolysis of F₂—M complexes produces closed-shell products involving two F atoms and M molecule. For example, F₂O can be formed by photolysis of F₂—O₃ complexes:



The second reaction channel involves reaction of one translationally excited F atom (produced from photodissociation of isolated F₂ molecule) with an isolated O₃ molecule, forming the complex FO—O₂. Our conclusion, that these two reaction products are formed from photolysis of different photoprecursors, is confirmed by the fact that an accumulation of F₂O and FO—O₂ occurs with different characteristic photochemical reaction rates (see Figure 3). The quantum yield for photodissociation of F₂ in solid argon at 355 nm is 0.35–0.5.¹⁵ On the basis of the ratio of photochemical reaction rates forming FO—O₂ and F₂O, the quantum yield for reaction 7 must be 0.5–0.7.

Table 2 shows the mass balance of consumption of O₃ molecules after exhaustive photolysis of the sample Ar:F₂:O₃ = 5000:3:1 at 15 K. This balance was determined from decrease of the O₃ band and from growth of the products bands which are shown in Figure 2. The relevant absorption coefficients are given in the next section. Table 2 shows that the consumption of ozone is somewhat greater than the concentrations of products F₂O and FO—O₂. The difference, 0.077, attributed to photolysis of clusters and aggregates O₃ in reaction 1. This value is consistent with the consumption of O₃ (~0.10) after photolysis of mixtures Ar/O₃ (see Figure 1).

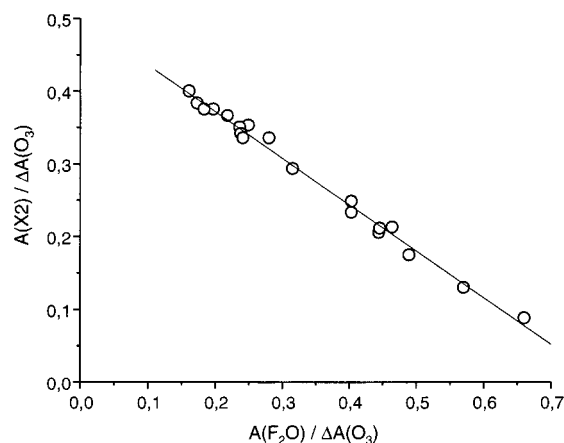
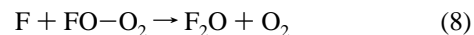


Figure 8. Intensities of the product bands normalized by the change in intensity of the reactant O₃(ν₃) band. Data points represent changes following annealing cycles at temperatures *T* > 20 K. All spectra were recorded at 15 K.

b. Reactions of Thermal F Atoms. The main process involving diffusing atoms at *T* > 20 K is reaction 4, which produces the strongly interacting stabilized FO—O₂ complexes. The quadratic dependence of the F₂O concentration with respect to the primary product, as shown in Figure 4, shows that F₂O is formed by addition of the second F atom to the primary FO—O₂ product:



We can make use of the aforementioned quadratic dependence between the concentrations of the primary and the secondary products to determine the infrared absorption cross sections of product bands, *B_i*, assuming that the observed consumption of ozone and formation of the complexes FO—O₂ and F₂O molecules is due entirely to reactions 4 and 8. Proceeding as before,¹⁹ we use the mass balance equation

$$\Delta[\text{O}_3] = [\text{FO}_3] + [\text{F}_2\text{O} + \text{O}_2] \quad (9)$$

to obtain a linear dependence between the integrated intensities of product bands, *A_{FO3}* and *A_{F2O}*, normalized by the corresponding decrease in intensity of the O₃(ν₃) band (Δ*A_{O3}*):

$$\frac{A_{\text{FO}_3}}{\Delta A_{\text{O}_3}} = -\beta_1 \frac{\Delta A_{\text{F}_2\text{O}}}{\Delta A_{\text{O}_3}} + \beta_2 \quad (10)$$

where $\beta_1 = B_{\text{FO}_3}/B_{\text{F}_2\text{O}}$ and $\beta_2 = B_{\text{FO}_3}/B_{\text{O}_3}$. Figure 8 shows a plot of the intensity of the X2 band of the complex FO—O₂ vs intensity of the F₂O band, both of which have been normalized to the corresponding change in the O₃ band intensities. These points were obtained during an extended annealing period of the sample. The points at small values of the abscissa correspond to short annealing times, when the product is mainly FO—O₂, and those at large values correspond to long annealing times. There is a linear dependence between the normalized intensities of product bands over a wide range of relative concentrations, as follows from eq 10. Such a linear dependence, corresponding to the mass-balance eq 9, confirms our conclusion that the main channel leading to O₃ consumption in the dark at *T* > 20 K is reaction 4. The relative absorption cross sections were determined from Figure 8 and eq 10 to be $B_{\text{FO}_3}(\text{X2})/B_{\text{F}_2\text{O}} = 0.65$ and $B_{\text{FO}_3}(\text{X2})/B_{\text{O}_3} = 0.50$. Using values for *B_{O3}*(ν₃), the integrated cross sections are $B_{\text{FO}_3}(\text{X2}) = 38 \pm 4$ km/mol for the F—O band in the complex FO—O₂ and $B_{\text{F}_2\text{O}} = 59 \pm 6$ km/

mol for the ν_3 band of the F₂O molecule. The last value is in good agreement with that calculated previously for the ν_3 band of the F₂O molecule, 53 ± 6 km/mol.³⁵ From the relative intensities of the X1 and X2 bands of the complex FO–O₂, we have determined the integrated cross section $B_{\text{FO}_3}(\text{X1}) = 55 \pm 5$ km/mol for the O–O band of the complex.

In section 3d, we estimated that the absorption cross section for the F–O band in the complex is ~ 3 times stronger than that for isolated FO radical. From the determined value $B_{\text{FO}_3}(\text{X2}) \approx 38$ km/mol, it follows that the absorption cross section for isolated FO radical should be $B_{\text{FO}} \approx 13$ km/mol. We have not found any experimental data in the literature about the absorption cross section for FO. Recent calculations³⁶ have predicted the value $B_{\text{FO}} = 27$ km/mol, which is twice as large as our estimate. Such a discrepancy could be due to the presence of other reaction channels for photodecomposition of the complex FO–O₂, which do not give isolated FO. Conversely, it could simply be an overestimated value obtained in the calculations.³⁶ Nevertheless, our results indicate that the absorption cross section for the F–O band in the complex is much higher than that in free FO.

5. Conclusions

The main experimental result of the present study is that the reaction both of translationally excited (at $T = 15$ K) and thermal F atoms (at $T > 20$ K) with ozone molecules in solid argon produces the strongly interacting stabilized complex FO–O₂. Kinetic analysis and IR spectra of isotopically enriched (¹⁶O and ¹⁸O) samples allow to point out the following characteristics of the stabilized complex.

The observed complex is characterized by two intense infrared bands at 1522 cm^{-1} (O–O stretch) and 968 cm^{-1} (F–O stretch).

The bands are red-shifted by 34 cm^{-1} from the corresponding gas-phase value for O₂(³Σ) and by 61 cm^{-1} from the matrix value for isolated FO(²Π) free radical.

The absorption cross sections are 55 ± 5 km/mol for 1522 cm^{-1} and 38 ± 4 km/mol for 968 cm^{-1} . The absorption cross section for the F–O band in the complex is much higher than that for the isolated FO free radical.

Photolysis by visible laser light 532 nm leads to decay of the complexes FO–O₂ and to the appearance of FO at 1029 cm^{-1} .

These properties demonstrate conclusively that the detected complex cannot be assigned to a weak van der Waals complex FO⋯O₂. They are strongly suggestive of an asymmetrical FO–O₂ association complex, which is formed by addition of an F atom to a terminal oxygen atom of the O₃ molecule. We believe that these data could serve as a starting point for quantum chemistry calculations in an effort to understand the bonding origin of such a complex and the topology of the potential energy surface in the vicinity of the transition state of atom–molecular chemical reactions type $\text{F} + \text{O}_3$. Ab initio calculations aimed to obtain the structure of the FO₃ complex having the

observed properties are now being carried out in both laboratories, in the USA and in Russia.

Acknowledgment. This research is supported by the National Science Foundation under Grant CHE-9526277.

References and Notes

- (1) Rollefson, G. K.; Byrns, A. C. *J. Am. Chem. Soc.* **1934**, *56*, 364.
- (2) Norrish, R. G. W.; Neville, J. H. *J. Chem. Soc.* **1934**, 1864.
- (3) Wongdontry-Stuper, W.; Jayanty, R. K. M.; Simonaitis, R.; Heicklen, J. *J. Photochem.* **1979**, *10*, 163.
- (4) Prasad, S. S.; Adams, W. M. *J. Photochem.* **1980**, *13*, 234.
- (5) Adams, W. M. *Nature* **1980**, *285*, 152.
- (6) Baulch, D. L.; Cox, R. A.; Crutzen, P. J.; Hampson, R. F., Jr.; Kerr, J. A.; Troe, J.; Watson, R. T. *J. Phys. Chem. Ref. Data* **1982**, *11*, 327.
- (7) Nicovich, J. M.; Kreutter, K. D.; Wine, P. H. *Int. J. Chem. Kinet.* **1990**, *22*, 399.
- (8) Zhang, J.; Lee, Y. T. *J. Phys. Chem. A* **1997**, *101*, 6485.
- (9) Grothe, H.; Willner, H. *Angew. Chem., Int. Ed. Engl.* **1994**, *33*, 1482.
- (10) Carter, III, R. O.; Andrews, L. *J. Phys. Chem.* **1981**, *85*, 2351.
- (11) Rauk, A.; Tschuikov-Roux, E.; Chen, Y.; McGrath, M. P.; Radom, L. *J. Phys. Chem.* **1993**, *97*, 7947.
- (12) Zhang, J.; Miao, T.-T.; Lee, Y. T. *J. Phys. Chem. A* **1997**, *101*, 6922.
- (13) Kieninger, M.; Segovia, M.; Ventura, O. N. *Chem. Phys. Lett.* **1998**, *287*, 597.
- (14) Kunntu, H.; Feld, J.; Alimi, R.; Becker, A.; Apkarian, V. A. *J. Chem. Phys.* **1990**, *92*, 4856.
- (15) Feld, J.; Kunntu, H.; Apkarian, V. A. *J. Chem. Phys.* **1990**, *93*, 1009.
- (16) Misochko, E. Ya.; Benderskii, A. V.; Wight, C. A. *J. Phys. Chem.* **1996**, *100*, 4496.
- (17) Misochko, E. Ya.; Benderskii, V. A.; Goldschleger, A. U.; Akimov, A. V.; Benderskii, A. V.; Wight, C. A. *J. Chem. Phys.* **1997**, *106*, 3146.
- (18) Goldschleger, A. U.; Misochko, E. Ya.; Akimov, A. V.; Goldschleger, I. U.; Benderskii, V. A. *Chem. Phys. Lett.* **1997**, *267*, 288.
- (19) Misochko, E. Ya.; Akimov, A. V.; Wight, C. A. *Chem. Phys. Lett.* **1998**, *293*, 547.
- (20) Misochko, E. Ya.; Akimov, A. V.; Goldschleger, I. U.; Boldyrev, A. I.; Wight, C. A. *J. Am. Chem. Soc.* **1999**, *121*, 405.
- (21) Brosset, P.; Dahoo, R.; Gauthier-Roy, B.; Abouaf-Marguin, L.; Lakhilfi, A. *Chem. Phys.* **1993**, *172*, 315.
- (22) Benderskii, A. V.; Wight, C. A. *J. Chem. Phys.* **1994**, *101*, 292.
- (23) Wight, C. A.; Misochko, E. Ya.; Vetoshkin, E. V.; Goldanskii, V. I. *Chem. Phys.* **1993**, *170*, 393.
- (24) Secroun, C.; Barbe, A.; Jouve, P.; Arcas, P.; Arie, E. *J. Mol. Spectrosc.* **1981**, *85*, 8.
- (25) Adler-Golden, S. M.; Langhoff, S. R.; Bauschlicher, Jr., C. W.; Carney, G. D. *J. Chem. Phys.* **1985**, *83*, 255.
- (26) Benderskii, A. V.; Wight, C. A. *Chem. Phys.* **1994**, *189*, 307.
- (27) Sedlacek, A. J.; Wight, C. A. *J. Phys. Chem.* **1989**, *93*, 509.
- (28) Griggs, M. J. *Chem. Phys.* **1968**, *49*, 857.
- (29) Vaida, V.; Donaldson, D. J.; Strickler, S. J.; Stephens, S. L.; Birks, J. W. *J. Phys. Chem.* **1989**, *93*, 506.
- (30) Arkell, A. J. *Phys. Chem.* **1969**, *73*, 3877.
- (31) Andrews, L.; Raymond, J. I. *J. Chem. Phys.* **1971**, *55*, 3078.
- (32) Andrews, L. *J. Chem. Phys.* **1972**, *57*, 51.
- (33) Huber, K. P.; Herzberg, G. *Molecular Spectra and Molecular Structure IV. Constants of Diatomic Molecules*; Van Nostrand Reinhold: New York, 1979.
- (34) Jacox, M. E. *J. Mol. Spectrosc.* **1980**, *84*, 74.
- (35) Tiel, W.; Scuseria, G.; Schaefer III, H. F.; Allen, W. D. *J. Chem. Phys.* **1988**, *89*, 4965.
- (36) McGrath, M. P.; Rowland, F. S. *J. Phys. Chem.* **1996**, *100*, 4815.